

Heterogeneous & Homogeneous & Bio- & Nano-

CHEMCATCHEM

CATALYSIS

Accepted Article

Title: Bifunctional Hierarchical Zeolite-Supported Silver Catalysts for the Conversion of Glycerol to Allyl Alcohol

Authors: Giacomo M Lari, Zupeng Chen, Cecilia Mondelli, and Javier Pérez-Ramírez

This manuscript has been accepted after peer review and appears as an Accepted Article online prior to editing, proofing, and formal publication of the final Version of Record (VoR). This work is currently citable by using the Digital Object Identifier (DOI) given below. The VoR will be published online in Early View as soon as possible and may be different to this Accepted Article as a result of editing. Readers should obtain the VoR from the journal website shown below when it is published to ensure accuracy of information. The authors are responsible for the content of this Accepted Article.

To be cited as: *ChemCatChem* 10.1002/cctc.201601635

Link to VoR: <http://dx.doi.org/10.1002/cctc.201601635>

WILEY-VCH

www.chemcatchem.org



Bifunctional Hierarchical Zeolite-Supported Silver Catalysts for the Conversion of Glycerol to Allyl Alcohol

Giacomo M. Lari, Zupeng Chen, Cecilia Mondelli,* and Javier Pérez-Ramírez*

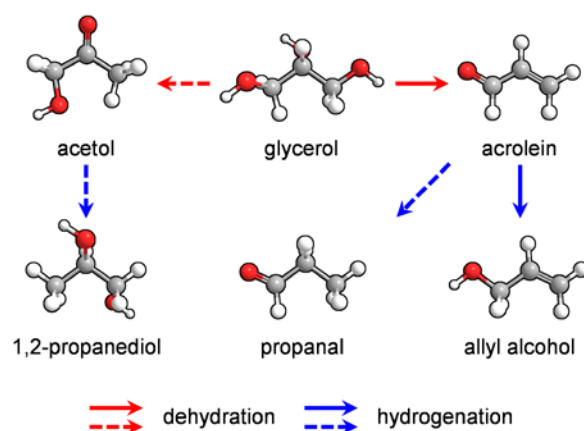
Abstract: The establishment of suitable processes for the conversion of glycerol into allyl alcohol is hindered by the fast deactivation of solid acids in the dehydration of the substrate to acrolein and by the requirement of hydrogen donors to enhance the selectivity of the subsequent reduction step. In this work, silver nanoparticles deposited onto a hierarchical ZSM-5 zeolite prove as an effective bifunctional catalyst to conduct the two reactions in the gas phase and in the presence of hydrogen using a continuous fixed-bed reactor. The acidic function was accomplished using a ZSM-5 zeolite modified by facile alkaline and acid treatments, which decreased the amount of Lewis-acid centers while preserving the amount of Brønsted-acid centers, and introduced an auxiliary network of intracrystalline mesopores, thus boosting the selectivity to acrolein (62%) and the resistance to coking. Upon screening of various metals supported onto the aluminosilicate, silver was identified as a superior hydrogenation phase, enabling a relatively high activity with a >50% allyl alcohol selectivity. Tuning of the metal loading, temperature, pressure, and contact time led to 15% yield of allyl alcohol, thus approaching the state-of-the-art transfer hydrogenation systems, and stable behavior for 100 h on stream. Our results highlight the advantage of conducting the two transformations over a bifunctional material rather than over two separate single-function solids.

Introduction

The development of chemocatalytic technologies to convert biomass into chemicals continues to receive great attention as a means to limit our reliance on fossil sources. In this context, glycerol, the main by-product in the manufacture of biodiesel, comprises a versatile starting material for the preparation of various compounds possessing a C₃ backbone.^[1] Besides the widely studied acrylates, lactates, carbonates, diols, *etc.*,^[2] few works have focused on allyl alcohol, which is a high added-value chemical used for the synthesis of specialty polymers, glycidol, glycidyl esters, and amines.^[3] Since its industrial production is based on the hydrogenation of propene-derived acrolein^[4] and the latter can be attained from glycerol through dehydration,^[5] a two-step transformation has been proposed to form allyl alcohol from the triol (Scheme 1).^[6]

In the initial dehydration, two water molecules are removed from glycerol, typically in the gas phase.^[7] Specifically, the secondary hydroxyl group of the substrate is protonated and eliminated, leading to the formation of 3-hydroxypropanal, which is quickly converted into acrolein under the conditions ($T > 450$ K) employed.^[7] Brønsted-acid sites have been identified as selective while Lewis-acid and basic functionalities alternatively activate the primary hydroxyl group, hence forming hydroxyacetone.^[5] Thus, strong solid acids, like heteropolyacids, sulfated zirconia, and zeolites, belong to the state-of-the-art heterogeneous catalysts.^[8] In particular, microporous crystalline aluminosilicates have been the materials of choice, since the possibility to tune their porous properties enables to address one of the main drawbacks of this reaction, *i.e.* fouling, which is due to the high reactivity of the reactant, intermediate, and product at the reaction temperature.^[9] Indeed, different approaches have been applied to increase the mesoporous surface of zeolites, which has been demonstrated as the main parameter correlating with lifetime in coke-forming reactions.^[10] Amongst these, post-synthetic modification *via* alkaline treatment led to mesoporous crystals with improved durability.^[10a] However, due to the increase in Lewis acidity upon desilication, the selectivity to acrolein was reduced in favor to that to acetol.

The selective hydrogenation of acrolein to allyl alcohol is particularly challenging due to the π -conjugation of the C=O bond with the C=C bond. Palladium, ruthenium, rhodium, and platinum are fully selective to propanal,^[11] while silver and gold catalysts show an allyl alcohol selectivity of 50–60% in gas-phase experiments.^[12] Alloying of silver with cadmium and zinc



Scheme 1. Simplified reaction network for the transformation of glycerol into allyl alcohol (solid arrows) and the main side products (dashed arrows).

G. M. Lari, Dr. Z. Chen, Dr. C. Mondelli,*
 Prof. Dr. J. Pérez-Ramírez*
 Institute for Chemical and Bioengineering
 Department of Chemistry and Applied Biosciences
 ETH Zurich
 Vladimir-Prelog-Weg 1, 8093 Zurich (Switzerland)
 E-mails: cecilia.mondelli@chem.ethz.ch, jpr@chem.ethz.ch

FULL PAPER

increased the yield up to 70% and this technology is industrially exploited.^[11c] In addition to the nature of the metal, the support was shown to have great effect on its performance, as the deposition of platinum on a strongly acidic carrier increased the allyl alcohol selectivity to 60%.^[11b] Transfer hydrogenation in the liquid phase has been proposed as an alternative for the preparation of allyl alcohol, using isopropanol and 2-butanol over Cd-Zn, MgO-ZnO, or lanthanide-based catalysts.^[13] While this approach slightly enhanced the selectivity, the generation of low-value ketones from the alcohols in equimolar amount to allyl alcohol represents a strong drawback toward an industrial process.

The combination of the two reactions over a single catalyst has been tackled infrequently and was typically performed in the presence of an organic hydrogen donor. Bulk and ceria-supported rhenium catalysts achieved high allyl alcohol yields in batch liquid-phase tests with pentanols or benzyl alcohol.^[14] Nevertheless, the scarce availability and extremely high price of this metal strongly limit the future commercialization of these materials. More viable systems include platinum or iron oxide supported onto an acidic carrier, which featured allyl alcohol yields of 10 or 20%, respectively, in the presence of propanols as hydrogen donors.^[15] Nevertheless, by-products formation and the loss of part of the donor due to dehydration over the acidic material emerged as additional disadvantages to the formation of the ketones. It should be noted that, although the production of allyl alcohol in the presence of molecular hydrogen has never been addressed directly, a yield of 5% in this chemical has been observed over copper or nickel on solid acids, which were used to transform glycerol into propan(di)ol.^[16]

Herein, we introduce silver nanoparticles supported on a hierarchical zeolite as an efficient bifunctional catalyst for the H₂-mediated transformation of glycerol into allyl alcohol in a continuous gas-phase process. The catalyst design firstly encompassed the tailoring of the porous and acidic properties of MFI-type aluminosilicates through post-synthetic base and acid treatments to increase their selectivity and long-term stability in the dehydration of the substrate to acrolein. Secondly, different metals deposited onto the optimized zeolite were tested to identify the best hydrogenation phase for the reduction of the intermediate to allyl alcohol. Thereafter, the supporting procedure and the metal loading were tuned along with the operating conditions to boost the productivity and on-stream durability of this novel catalytic technology.

Results and Discussion

Design of the dehydration phase

The development of suitable catalysts for the conversion of glycerol into allyl alcohol in the presence of molecular hydrogen involved the design of acid and redox components. Based on its previous preferred use in this reaction,^[10a,17] a commercially available zeolite with MFI framework topology and a nominal bulk Si/Al = 40 (coded as H-Z40) was selected for the first phase and modified through post-synthetic treatments to enhance its stability

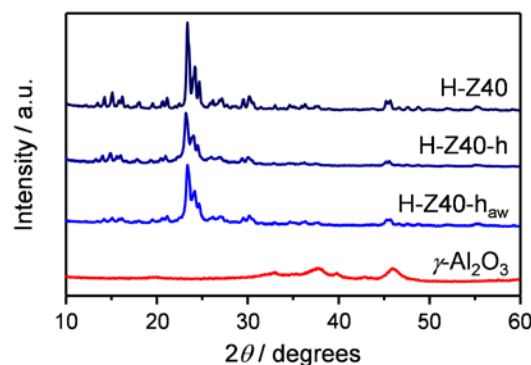


Figure 1. X-ray diffractograms of the acid catalysts investigated.

and selectivity towards the acrolein intermediate. The former property was improved contacting the aluminosilicate with 0.3 M aqueous NaOH, which leads to the extraction of silicon atoms from the framework, generating a secondary network of interconnected mesopores.^[18] Upon this treatment, the Si/Al ratio decreased to 26 (H-Z40-h, **Table 1**), the mesoporous surface area increased to 303 m² g⁻¹, and ca. 45% of the initial crystallinity (**Figure 1**) and 31% of the original microporous volume were lost. In spite of the lower Si/Al ratio, the overall density of acid sites (**Table 1**) as well as the Brønsted-/Lewis-acid sites ratio decreased, in agreement with previous observations that a good fraction of the aluminum atoms in the modified zeolite are present in the form of hexacoordinated species with Lewis-acid character.^[19] To remove these unselective sites, an acid washing was performed, which produced H-Z40-h_{aw}. This step decreased the aluminum content by ca. 25%. Coherently with the removal of amorphous portions of the material, the microporous volume of the zeolite was partially (by ca. 10%) restored and the Lewis acidity halved, while the Brønsted acidity remained unchanged. The parent and modified zeolites were tested in the gas-phase conversion of glycerol at 673 K for 2 h on stream. As expected, the selectivity to acrolein was found to depend on the Brønsted acidity of the materials (**Figure 2a**), being 49.2, 31.8, and 62.1% for H-Z40, H-Z40-h, and H-Z40-h_{aw}, respectively. Acetol and coke formed as by-products (**Table 2**), as indicated in earlier literature reports, while compounds that could originate from oxidation and reduction reactions were not observed, in line with the very modest activity of aluminosilicates in these transformations and the inert atmosphere employed.^[20] The extent of acetol generation followed the Lewis acidity of the zeolites: H-Z40-h > H-Z40 > H-Z40-h_{aw}. The role of this property was confirmed by testing Lewis-acidic γ -alumina, which displayed the highest selectivity to this chemical. The behavior of H-Z40, H-Z40-h, and H-Z40-h_{aw} was investigated over prolonged runs (**Figure 2b**). In line with previous studies indicating an augmented S_{meso} as the main parameter determining catalyst lifetime in this reaction,^[10a] the modified zeolites displayed higher stability than H-Z40. Nevertheless, H-Z40-h exhibited a lower deactivation rate than H-Z40-h_{aw}. These results can be rationalized considering that, in

FULL PAPER

Table 1. Characterization data for the acid and bifunctional catalysts.

Catalyst	M^a wt. %	Si/Al ^a mol mol ⁻¹	Na ^a wt. %	S_{BET}^b m ² g ⁻¹	S_{meso}^c m ² g ⁻¹	V_{pore}^d cm ³ g ⁻¹	V_{micro}^c cm ³ g ⁻¹	Cryst. ^e %	C_a^f μmol g ⁻¹	C_L^f μmol g ⁻¹
γ-Al ₂ O ₃	-	0	0.0	85	83	0.50	0.00	-	4	81
H-Z40	-	42	0.4	397	97	0.26	0.16	100	177	63
H-Z40-h	-	26	0.4	518	303	0.78	0.11	55	126	67
H-Z40-h _{aw}	-	45	0.4	594	366	0.90	0.12	62	142	37
Pd/H-Z40-h _{aw}	6.8	40	2.7	467	298	0.76	0.09	59	121	51
Pt/H-Z40-h _{aw}	6.0	43	0.6	481	320	0.79	0.08	64	130	60
Au/H-Z40-h _{aw}	6.9	43	0.3	544	337	0.81	0.11	61	145	64
Ru/H-Z40-h _{aw}	5.7	44	0.6	541	335	0.85	0.11	58	129	59
Ag/H-Z40-h _{aw}	2.7	43	0.3	523	339	0.86	0.10	60	120	65

^a XRF. ^b BET method. ^c *t*-plot method. ^d Volume adsorbed at $p/p_0 = 0.99$. ^e XRD, with respect to H-Z40. ^f FTIR of adsorbed pyridine.

spite of a larger S_{meso} , the latter solid has a slightly higher concentration of Brønsted-acid sites, which are known to favor condensation reactions leading to coke.^[21] Thus, they suggest that the density of strong acid sites is an additional parameter

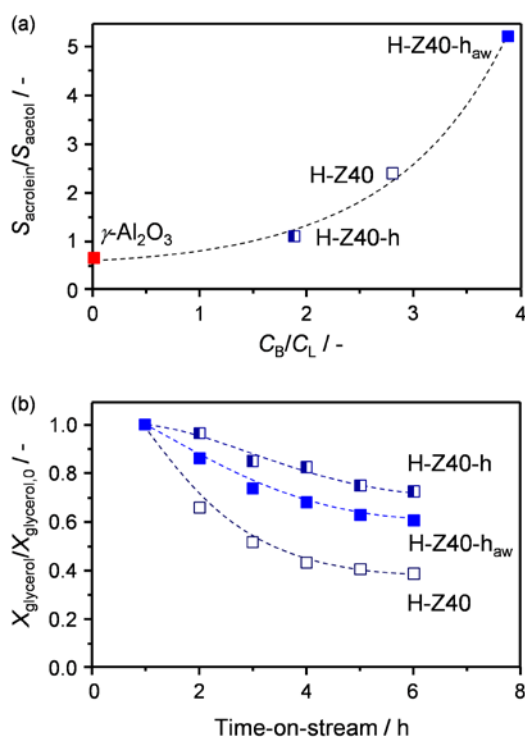


Figure 2. (a) Acrolein to acetol selectivity ratio versus the relative concentration of Brønsted- and Lewis-acid sites and (b) temporal evolution of the normalized conversion of glycerol over the dehydration catalysts investigated.

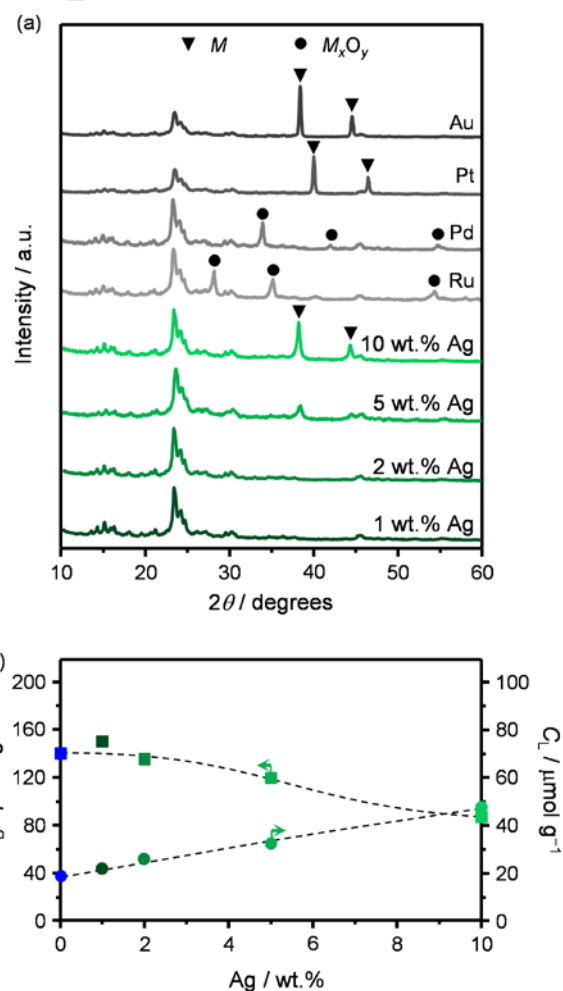


Figure 3. (a) X-ray diffractograms of the bifunctional catalysts studied and (b) concentration of Brønsted- and Lewis-acid sites versus the Ag content.

FULL PAPER

Table 2. Performance acid and bifunctional catalysts in the gas-phase conversion of glycerol.

Catalyst	X_{glycerol} %	S_{acetol} %	$S_{1,2\text{-propanediol}}$ %	$S_{\text{allyl alcohol}}$ %	S_{propanal} %	S_{acrolein} %	Coke ^a wt. %	CB ^b %
$\gamma\text{-Al}_2\text{O}_3$	24.1	51.7	0.1	0.0	0.0	22.8	0.8	93.9
H-Z40	34.8	28.8	1.0	0.1	0.0	49.2	2.1	90.6
H-Z40-h	48.2	40.2	1.4	0.1	0.0	31.8	3.4	90.1
H-Z40-h _{aw}	52.2	16.4	0.8	0.0	0.0	62.1	2.7	89.1
5% Pd/H-Z40-h _{aw}	73.0	34.9	10.8	6.2	36.8	11.4	1.1	100.5
5% Pt/H-Z40-h _{aw}	84.2	10.1	15.4	7.7	40.9	21.2	0.5	96.5
5% Au/H-Z40-h _{aw}	21.0	20.1	2.4	4.1	0.8	67.6	0.9	99.9
5% Ru/H-Z40-h _{aw}	18.7	15.1	7.4	8.1	14.9	20.2	1.2	95.1
5% Ag/H-Z40-h _{aw}	53.5	15.1	8.0	13.1	10.6	47.4	0.8	96.9

^a TGA, determined after 2 h reaction. ^b Carbon balance. Samples were collected between 1 and 2 h on stream.

determining the on-stream performance. Based on its superior selectivity to acrolein, H-Z40-h_{aw} was selected for further investigations.

Design of the hydrogenation phase

Various metals (Pt, Ru, Pd, Ag, and Au) were chosen based on the literature dealing with the selective hydrogenation of acrolein to allyl alcohol and deposited onto H-Z40-h_{aw} by incipient wetness impregnation in an amount corresponding to a 5 wt.% loading. Elemental analysis (**Table 1**) revealed that the metal content was close to the nominal value in all cases and that the composition of the support was not affected by the catalyst preparation procedure. X-ray diffraction (XRD, **Figure 3a**) evidenced the presence of metallic phases for Ag-, Au-, and Pt-based solids and of metal oxides for Pd- and Ru-containing catalysts. In all cases, the Brønsted acidity of the synthesized materials slightly diminished (<15% variation, **Table 1**), while the concentration of Lewis-acid sites increased substantially.

The zeolite-supported metal catalysts were tested in the gas-phase conversion of glycerol at 673 K in the presence of hydrogen (40 bar). In line with the decrease of the Brønsted-/Lewis-acid sites ratio upon metal deposition, the relative acrolein/acetol selectivity slightly decreased (**Table 2**). To corroborate the importance of the preservation of the active acid sites of the support during the incorporation of the metal phase, an alternative synthesis procedure was applied, in which the metal precursor was reduced by addition of NaBH₄ after impregnation. In fact, hydride ions strongly react with protons at the zeolite surface, leading to the exchange of protonic sites with sodium. Due to its poor Brønsted (15 $\mu\text{mol g}^{-1}$) and moderate Lewis (83 $\mu\text{mol g}^{-1}$) acidity, this material displayed a low glycerol conversion (24.6%) and a high acetol selectivity (78.3%). Regarding the hydrogenation activity, part of both the acetol and acrolein formed were converted into 1,2-propanediol and into allyl alcohol and

propanal, respectively. While the selectivity towards the diol lied in a relatively narrow range for all of the catalysts studied, the choice of the metal and of the loading was demonstrated crucial to balance between the desired hydrogenation of acrolein to allyl alcohol and its undesired reduction to propanal. In agreement with some previous reports,^[11] the use of palladium and platinum generated catalysts that converted acrolein to propanal with almost full selectivity (86 and 84% based on the amount of acrolein converted) and a relatively high activity. Conversely, gold ruthenium, and silver exhibited a relatively low hydrogenation activity, but much higher selectivity. In particular, silver provided

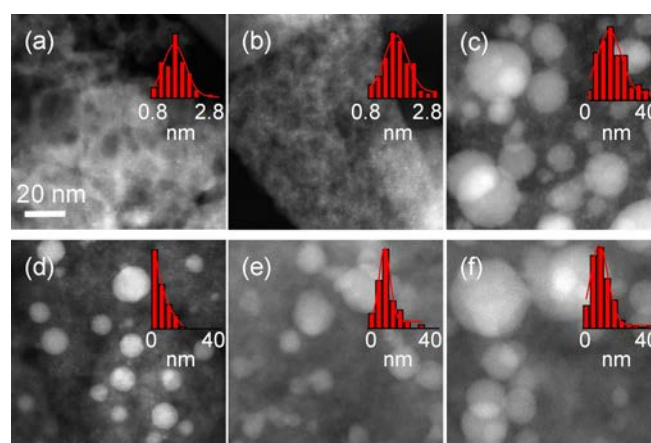


Figure 4. TEM micrographs and corresponding particle size distributions of the (a) 1, (b) 2, and (c) 10 wt.% Ag/H-Z40-h_{aw} catalysts and of the 5 wt.% Ag/H-Z40-h_{aw} catalyst (d) as-prepared, (e) reduced, and (f) after use.

FULL PAPER

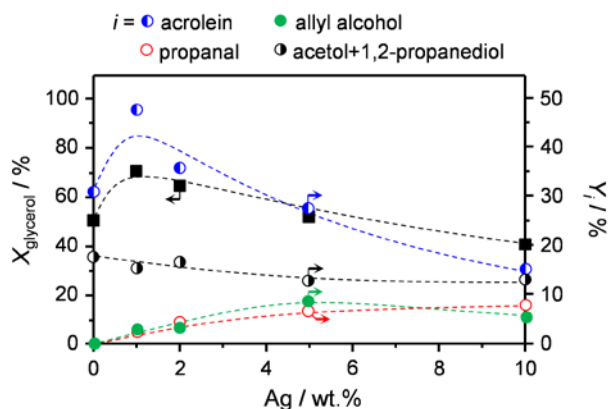


Figure 5. Glycerol yield and product selectivity versus the Ag loading of the H-Z40-_{haw}-supported catalysts.

the highest allyl alcohol yield (13.1% at 53.5% glycerol conversion), which was further optimized by tuning of its metal loading. For this purpose, additional catalysts with a metal content in the 1-10 wt.% range were prepared. When the silver loading was lower than 5 wt.%, the reflections at $2\theta = 38.2$ and 44.4° , assigned to the (111) and (200) lattice planes of Ag, were not detected (**Figure 3a**), pointing to a high dispersion of the metal. The latter was supported by high-angle annular dark field scanning transmission electron microscopy (HAADF-STEM, **Figure 4**). Only small Ag clusters (ca. 1-2 nm) were visualized in the as-prepared 1 and 2 wt.% Ag/H-Z40-_{haw} catalysts (**Figure 4a** and **b**), while particles of ca. 10 nm were visible in the 10 wt.% Ag/H-Z40-_{haw} sample (**Figure 4c**). A broad particle size distribution, featuring small silver clusters and larger aggregates, was measured for the as-prepared 5 wt.% Ag/H-Z40-_{haw} (**Figure 4d**). Onto this material, further clustering was observed after reduction with hydrogen (**Figure 4e**). This indicates that the particle size depended on both the metal loading and the conditions to which the catalysts were subjected. Investigation of the acidic properties of these solids revealed a moderate depletion of the density of Brønsted sites (**Table 1**) and an increase in the concentration of Lewis centres with respect to the bare zeolite. These effects likely arose from the ion exchange of some of the acidic protons with Ag cations upon impregnation of the precursor. Although most of these are displaced from these positions and reduced to nanoparticles, a part proportional to the metal loaded remains in its Lewis-acidic cationic form at the expense of part of the protons (**Figure 3b**). Higher and lower silver contents did not lead to better performances. In fact, at higher metal loadings (**Figure 5**), the increased selectivity of the hydrogenation reaction originating from the larger amount of metal centres was counterbalanced by the lower formation of the dehydration product to be reduced, *i.e.*, acrolein. The latter likely arose from the decrease of the acidity and accessibility of portions of the zeolite crystals due to the bulky metal particles blocking the pores. At lower silver loadings, the situation was reversed, *i.e.*, more acrolein was formed but it could be hardly transformed into allyl alcohol due to the insufficient amount of redox centres. The catalytic performance was optimized by tuning the temperature,

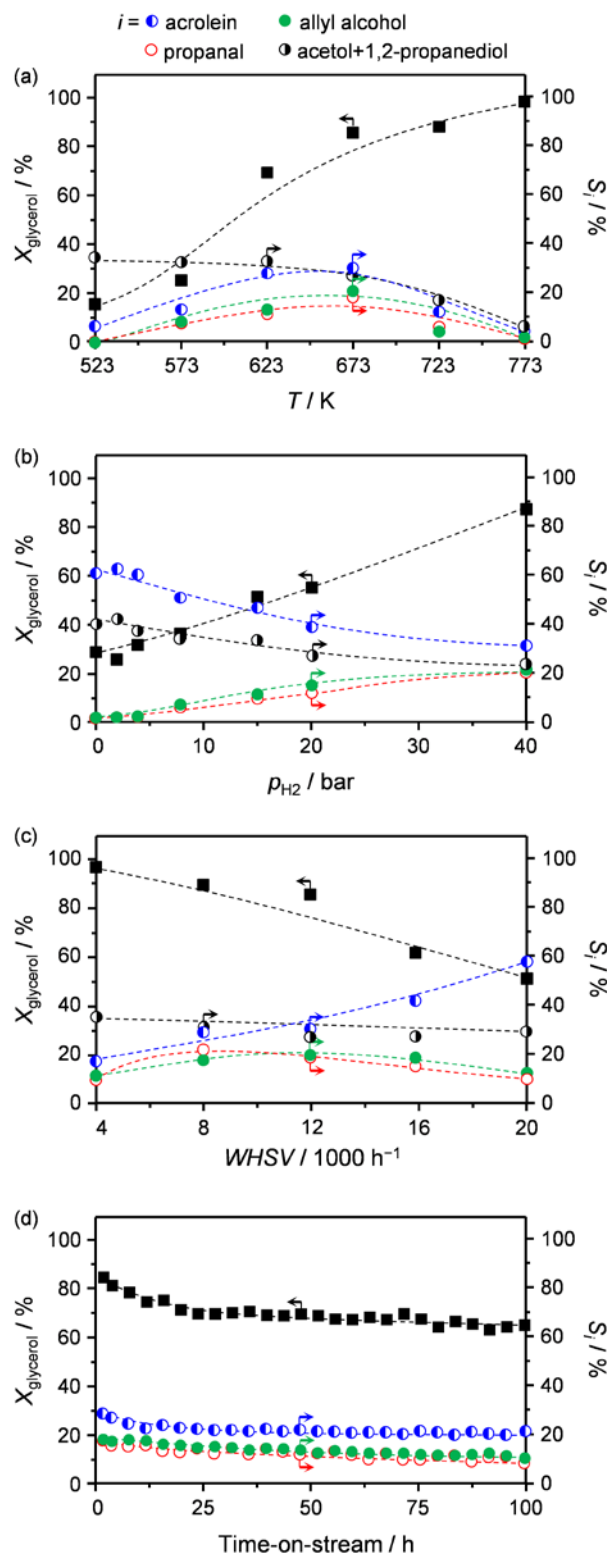


Figure 6. Glycerol conversion and product selectivity over 5 wt.% Ag/H-Z40-_{haw} versus the (a) temperature, (b) pressure, (c) weight hourly space velocity, and (d) time-on-stream.

FULL PAPER

pressure, and space velocity. With respect to the first parameter, the conversion was moderate at low values and monotonously incremented at progressively higher temperatures, reaching 100% at 773 K (**Figure 6a**). The selectivity to acrolein and to its hydrogenation products increased up to 673 K and then diminished at higher temperatures. Under the latter conditions, a low value was determined for the mass balance, which was correlated with the stronger relevance of condensation, coking, and unselective hydrogenation reactions forming solid deposits on the catalyst surface. Based on these results, the hydrogen pressure was varied in the 0–40 bar range at 673 K (**Figure 6b**). In the absence of hydrogen, similar results were obtained as upon the use of H-Z40-h_{aw}, except for a slightly lower selectivity to acrolein, which was attributed to the decreased amount of strong acid sites. By raising the hydrogen pressure, the conversion augmented, as well as the selectivity to acrolein hydrogenation products. While the second observation is explained in a straightforward manner by the higher amount of hydrogen available for the transformation, the first is likely due to the fact that the acid sites required for the conversion of glycerol into acrolein are partly saturated by the adsorbed product and become more available when this is removed through reduction. Concerning the space velocity, the conversion was shown to decrease at higher values of this parameter, in line with the lower contact time between the reactants stream and the catalyst. In view of the consecutive nature of the dehydration and hydrogenation steps, the selectivity of the intermediates was enhanced and the one to the products depleted as a function of this variable (**Figure 6c**). Finally, the stability of the 5 wt.% Ag/H-Z40-h_{aw} was tested under the optimized reaction conditions for 100 h on stream (**Figure 6d**). The conversion and selectivity to acrolein moderately decreased during the first 24 h, which could be tentatively rationalized by the fact that part of the strong Brønsted-acid sites were poisoned with adsorbed species, thus altering the effective Brønsted/Lewis-acid sites ratio. In view of the reduced selectivity to acrolein, also the selectivity to allyl alcohol and propanal slightly decreased, although their ratio was constant. After this initial drop in performance, the behaviour of the catalyst remained stable till the end of the run. Microscopic analysis of the used catalyst revealed that the silver particle size did not change over the course of the reaction (**Figure 4f**). The increase in stability observed in this reaction as compared to the test with the zeolite only (**Figure 2b**) is remarkable and demonstrates that adding a hydrogenation functionality to the acid catalyst is effective in boosting its resistance. This is likely due to the reduction of coke precursor molecules produced by dehydration, as speculated in an earlier work,^[7] and is in line with the lower amount of coke detected on the catalyst after reaction (1.8 wt.%).

Conclusions

In this study, we uncovered silver nanoparticles supported onto a hierarchical ZSM-5 zeolite as an efficient bifunctional catalyst for the continuous dehydration-hydrogenation of glycerol into allyl alcohol in the gas-phase. The material was designed tuning the

acidic properties and porosity of a commercially available zeolite and selecting a suitable hydrogenation functionality. With respect to the aluminosilicate, alkaline treatment proved an easy tool to introduce an auxiliary network of intracrystalline mesopores, thus increasing the resistance to coking and providing longer lifetime in the dehydration of glycerol. Furthermore, a subsequent acid washing was effective in removing residual Lewis acidity, thus further raising the selectivity to acrolein. Silver was identified as a better hydrogenation phase than various noble metals based on its considerable activity in reducing acrolein and its remarkable selectivity to allyl alcohol in the presence of molecular hydrogen. The best catalyst, featuring a 5 wt.% Ag loading onto the zeolite, led to a selectivity to allyl alcohol of 20% at a glycerol conversion of 80% under optimized conditions of temperature, pressure, and contact time. Moreover, it displayed a minor activity loss upon a 100-h run. This was attributed to the ability of silver to hydrogenate coke precursors, which form on the surface under the reaction conditions and usually lead to a rapid blocking of the active sites. Our findings provide new insight into the parameters to be taken into account in the development of bifunctional catalysts for multistep biomass transformations, showing the synergistic effects that might arise from coupling components required for different reactions.

Experimental Section

Catalyst synthesis

NH₄-ZSM-5 with a Si/Al ratio of 40 was obtained from Zeolyst International (CBV8014, referred to as Z40) and was converted into the protonic form (H-Z40) by calcination at 823 K for 5 h (5 K min⁻¹). γ -Al₂O₃ (Alfa Aesar, 99.997%) was used as received.

Post-synthetic modification of Z40. H-Z40 was subjected to desilication in an aqueous NaOH solution (0.3 M, 30 min, 100 cm³ per gram of zeolite) at 338 K in an Easymax™ 102 reactor (Mettler Toledo). The resulting suspension was filtered and the material obtained was ion exchanged through three consecutive treatments in an aqueous NH₄NO₃ solution (0.1 M, 8 h, 100 cm³ per gram of zeolite) at room temperature. The solid was recovered by filtration, washed with deionized water (100 cm³ per gram of zeolite, three times), dried at 338 K for 16 h, and calcined at 823 K for 5 h (5 K min⁻¹). The sample was denoted as H-Z40-h. An aliquot of this powder was treated three times with HCl (0.1 M, 8 h, 100 cm³) at 338 K, filtered, washed with deionized water (100 cm³ per gram of zeolite, three times), and dried at 338 K. The sample obtained was denoted as H-Z40-h_{aw}. H-Z40-h (1 g) was further treated with an aqueous solution of NaBH₄ (0.05 M, 10 cm³, Sigma Aldrich, >98%) and dried (338 K, 16 h). This material was denoted as H-Z40-h_{NaBH₄}.

Metal incorporation. Supported metal (Pt, Ru, Pd, Ag, and Au) catalysts were prepared by incipient wetness impregnation. The desired amount of RuCl₃·xH₂O (ABCR-Chemicals, 99.9%), Na₂PdCl₄ (Aldrich-Fine Chemicals, 98%), AgNO₃ (ABCR-Chemicals, 99.9%), K₂PtCl₄ (Acros Organics, 99.99%), or HAuCl₄·3H₂O (Acros Organics, ≥49.0 wt.% Au) to obtain a 5 wt.% metal loading was dissolved in deionized water (same amount as the total pore volume of the support, measured by N₂ sorption) and added to the carrier (475 mg). The resulting powder was mixed thoroughly, dried at room temperature, and calcined using the protocol

FULL PAPER

described above. Ag/H-Z40-h_{aw} catalysts containing 1, 2, and 10 wt.% of the metal were additionally prepared following the same procedure.

Catalyst characterization

The metal content in the catalysts was determined by X-ray fluorescence spectroscopy (XRF) using a Orbis Micro XRF instrument equipped with a Rh source operated at 35 kV and 500 μ A. Powder X-ray diffraction (XRD) was performed using a PANalytical X'Pert PRO-MPD diffractometer with Ni-filtered Cu K α radiation ($\lambda = 0.1541$ nm), acquiring data in the 10–60° 2 θ range with an angular step size of 0.05° and a counting time of 2 s per step. The crystallinity of the zeolite in the catalysts was estimated from the ratio between the area of selected reflections (23.1, 24.0, and 24.4° 2 θ) of the modified and parent samples. N₂ sorption at 77 K was conducted using a Micromeritics TriStar analyzer. Prior to the measurements, the solids were degassed at 573 K under vacuum for 3 h. Fourier transform infrared spectroscopy (FTIR) of adsorbed pyridine was conducted using a Bruker IFS66 spectrometer equipped with a mercury-cadmium-telluride (MCT) detector. Wafers (ca. 1 cm², 20 mg) were degassed at 693 K under vacuum for 4 h, cooled to room temperature and exposed to pyridine vapors (Sigma-Aldrich, >99%). Thereafter, they were evacuated at room temperature (15 min) and at 473 K (30 min). Spectra were recorded in the 4000–1300 cm⁻¹ range by accumulation of 32 scans with a resolution of 4 cm⁻¹. The concentration of Brønsted- and Lewis-acid sites was determined by integration of the peaks at 1545 and 1455 cm⁻¹ using 1.67 and 2.22 cm² μ mol⁻¹ as the extinction coefficients, respectively.^[10c] Scanning transmission electron microscopy (STEM) was undertaken using a FEI TalosTM F200X microscope operated at 300 kV (field emission gun). The particle size distribution was determined by counting more than 100 particles and fitted by a Gaussian model. The samples were prepared by dusting the catalysts onto standard copper mesh holey carbon supported grids.

Catalytic testing

The gas-phase conversion of glycerol into allyl alcohol was studied in the 0.1–4.0 MPa pressure range in an Effi Microactivity Reactor (PID Eng&Tech) comprising: (i) mass flow controllers for feeding N₂ (PanGas, 99.999%) and H₂ (Messer, 99.999%), (ii) a high-performance liquid chromatography (HPLC) pump for the feeding of the glycerol solution (20 wt.% in water, Sigma-Aldrich), (iii) a tubular stainless steel micro-reactor (i.d. = 6 mm) heated in an oven, and (iv) a liquid-gas separator located downstream of the reactor and kept at 273 K. The catalyst (0.1 g, particle size = 0.2–0.4 mm) was loaded into the reactor and the system was heated to 673 K in N₂ flow (100 cm³ min⁻¹). Thereafter, the gas composition was changed to 20 vol.% H₂/N₂ for 2 h to reduce the catalyst. The temperature, pressure, and gas composition were modified to the desired reaction values and the system allowed to equilibrate for 30 min, before the liquid feed was admitted at a rate of 0.1 cm³ min⁻¹. Liquid samples were periodically collected at the liquid-gas separator and analyzed by HPLC using an Agilent 1260 system equipped with an HPX-87H column kept at 308 K and a refraction index detector. A 0.005 M aqueous H₂SO₄ solution flowing at 0.600 cm³ min⁻¹ was used as the eluent. Calibration curves were measured in the 0.1–20 wt.% range using glycerol (Sigma-Aldrich, 99%), acrolein (Fluka, >95%), allyl alcohol (Sigma-Aldrich, >99%), hydroxyacetone (Alfa Aesar, 95%), 1,2-propanediol (Acros Organics, 99%), propanol (Sigma-Aldrich, >99%), and propanal (Sigma-Aldrich, 97%). The conversion was calculated as the ratio between the

number of moles of glycerol reacted and the mole of glycerol fed, the selectivity to product *i* as the number of moles of product *i* formed per mole of glycerol reacted, and the yield of product *i* as the product between glycerol conversion and selectivity to product *i*. The carbon balance was calculated as the ratio between the number of moles of carbon in the condensate and the number of moles of carbon fed. The experimental error, determined on the basis of three repetitions under selected testing conditions, was within $\pm 5\%$.

Acknowledgements

This work was funded by the Swiss National Science Foundation (Projects 200020-159760 and 200021-169679). The Scientific Center for Optical and Electron Microscopy at ETH Zurich, ScopeM, is acknowledged for the use of its facilities. Ms. E. Vorobjeva is thanked for the STEM analyses.

Keywords: allylic compounds • glycerol valorization • hierarchical zeolites • hydrogenation • silver

- [1] M. Pagliaro, R. Cirimmina, H. Kimura, M. Rossi, C. Della Pina, *Angew. Chem. Int. Ed.* **2007**, *46*, 4434–4440.
- [2] a) M. Dolores Soriano, P. Concepción, J. M. López Nieto, F. Cavani, S. Guidetti, C. Trevisanut, *Green Chem.* **2011**, *13*, 2954–2962; b) Y. Shen, S. Zhang, H. Li, Y. Ren, H. Liu, *Chem. - Eur. J.* **2010**, *15*, 7368–7371; c) M. Aresta, A. Dibenedetto, F. Nocito, C. Pastore, *J. Mol. Catal. A: Chem.* **2006**, *257*, 149–153; d) A. Alhanash, E. F. Kozhevnikova, I. V. Kozhevnikov, *Catal. Lett.* **2008**, *120*, 307–311.
- [3] a) C. L. Rinsch, X. Chen, V. Panchalingam, R. C. Eberhart, J.-H. Wang, R. B. Timmons, *Langmuir* **1996**, *12*, 2995–3002; b) L. Harvey, E. Kennedy, B. Z. Dlugogorski, M. Stockenhuber, *Appl. Catal., A* **2015**, *489*, 241–246.
- [4] a) P. Claus, *Appl. Catal., A* **2005**, *291*, 222–229; b) K. Weissermel, H.-J. Arpe, *Industrial Organic Chemistry*, Wiley-VCH, Weinheim, **2008**, pp. 217–238.
- [5] B. Katryniok, S. Paul, F. Dumeignil, *ACS Catal.* **2013**, *3*, 1819–1834.
- [6] a) G. Sánchez, J. Friggieri, A. A. Adesina, B. Z. Dlugogorski, E. M. Kennedy, M. Stockenhuber, *Catal. Sci. Technol.* **2014**, *4*, 3090–3098; b) D. S. Kim, W. J. Lee, M. Kong, Y.-J. Choe, H. Nam, *US Pat.* 9120718, **2015**.
- [7] A. Alhanash, E. F. Kozhevnikova, I. V. Kozhevnikov, *Appl. Catal., A* **2010**, *378*, 11–18.
- [8] a) E. Tsukuda, S. Sato, R. Takahashi, T. Sodesawa, *Catal. Commun.* **2007**, *8*, 1349–1353; b) F. Cavani, S. Guidetti, L. Marinelli, M. Piccinini, E. Ghedini, M. Signoretto, *Appl. Catal., B* **2010**, *100*, 194–204;
- [9] A. Corma, G. W. Huber, L. Sauvanaud, P. O'Connor, *J. Catal.* **2008**, *257*, 163–171.
- [10] a) L. G. Possato, R. N. Diniz, T. Garetto, S. H. Pulcinelli, C. V. Santilli, L. Martins, *J. Catal.* **2013**, *300*, 102–112; b) C.-J. Jia, Y. Liu, W. Schmidt, A.-H. Lu, F. Schüth, *J. Catal.* **2010**, *269*, 71–79; c) M. Milina, S. Mitchell, N.-L. Michels, J. Kevlin, J. Pérez Ramirez, *J. Catal.* **2013**, *308*, 398–407; d) R. Srivastava, M. Choi, R. Ryoo, *Chem. Commun.* **2006**, 4489–4491.
- [11] a) B. Coq, F. Figueras, P. Geneste, C. Moreau, P. Moreau, M. Warawdekar, *J. Mol. Catal.* **1993**, *78*, 211–226; b) W. Grünert, A. Brückner, H. Hofmeister, P. Claus, *J. Phys. Chem. B* **2004**, *108*, 5709–5717; c) T. H. Vanderspurt, *US Pat.* 4072727, **1978**.
- [12] a) C. Mohr, H. Hofmeister, M. Lucas, P. Claus, *Chem. Eng. Technol.* **2000**, *12*, 324–328; b) M. Bron, D. Teschner, A. Knop-Gericke, F. C. Jentoft, J. Kröhnert, J. Hohmeyer, C. Volckmar, B. Steinhauer, R. Schlögl, P. Claus, *Phys. Chem. Chem. Phys.* **2007**, *9*, 3559–3569.

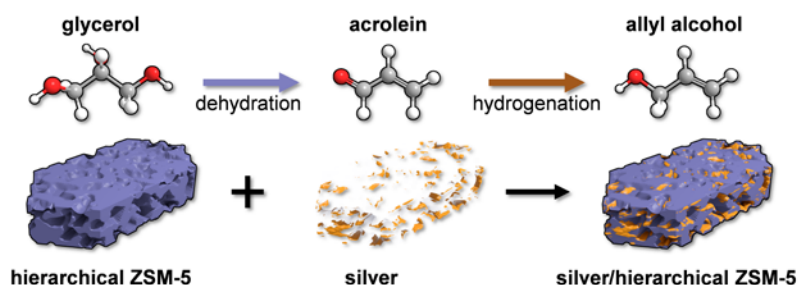
FULL PAPER

- [13] a) M. Gliński, U. Ulkowska, *Catal. Lett.* **2011**, *141*, 293-299; b) Y. Watanabe, M. Kurashige, *US Pat.* 5347056, **1994**; c) Y. Shimasaki, Y. Hino, M. Ueshima, *EU Pat.* 0183225, **1988**.
- [14] a) V. Canale, L. Tonucci, M. Bressan, N. d'Alessandro, *Catal. Sci. Technol.* **2014**, *4*, 3697-3704; b) C. Boucher-Jacobs, K. M. Nicholas, *ChemSusChem* **2013**, *6*, 597-599; c) J. Yi, S. Liu, M. M. Abu-Omar, *ChemSusChem* **2012**, *5*, 1401-1404.
- [15] a) I. Gandarias, P. L. Arias, J. Requies, M. B. Güemez, J. L. G. Fierro, *Appl. Catal., B* **2010**, *97*, 248-256; b) A. Konaka, T. Tago, T. Yoshikawa, A. Nakamura, T. Masuda, *Appl. Catal., B* **2014**, *146*, 267-273; c) E. Arceo, P. Marsden, R. G. Bergman, J. A. Ellman, *Chem. Commun.* **2009**, 3357-3359.
- [16] a) X. Lin, Y. Lv, Y. Xi, Y. Qu, D. L. Phillips, C. Liu, *Energy Fuels* **2014**, *28*, 3345-3351; b) L. Huang, Y. Zhu, H. Zheng, G. Ding, Y. Li, *Catal. Lett.* **2009**, *131*, 312-320.
- [17] S.-H. Chai, H.-P. Wang, Y. Liang, B.-Q. Xu, *Green Chem.* **2007**, *9*, 1130-1136.
- [18] J. C. Groen, J. A. Moulijn, J. Pérez-Ramírez, *J. Mater. Chem.* **2006**, *16*, 2121-2131.
- [19] S. Mitchell, M. Milina, R. Verel, M. Hernández-Rodríguez, A. B. Pinar, L. B. McCusker, J. Pérez-Ramírez, *Chem. - Eur. J.* **2015**, *21*, 14156-14164.
- [20] A. Corma, *Chem. Rev.* **1995**, *95*, 559-614.
- [21] D. Mores, J. Kornatowski, U. Olsbye, B. M. Weckhuysen, *Chem. - Eur. J.* **2011**, *17*, 2874-2284.

FULL PAPER

Entry for the Table of Contents

FULL PAPER



Giacomo M. Lari, Zupeng Chen, Cecilia Mondelli*, Javier Pérez-Ramírez*

Page 1 – Page 8

Bifunctional Hierarchical Zeolite-Supported Silver Catalysts for the Conversion of Glycerol to Allyl Alcohol

The conversion of glycerol into allyl alcohol is efficiently catalyzed by a bifunctional catalyst comprising silver nanoparticles supported on a hierarchical ZSM-5 zeolite. This material combines the high stability of the zeolite and the remarkable selectivity of the metal for the dehydration and hydrogenation steps, respectively.